ELECTROMAGNETIC RESONANCE BEHAVIOUR OF LHC VACUUM INTERCONNECT MODULES

H. R. Gobakken*, G. Bregliozzi, S. Calatroni, P. Chiggiato, P. Krkotić, I. Wevers
CERN, Geneva, Switzerland

Abstract

Beam-induced heating has become increasingly relevant for vacuum interconnect modules (VIMs) in the Large Hadron Collider (LHC) with the continuing rise in the beam intensity heightening their sensitivity to electromagnetic resonances. While the heating itself is not the primary subject of this work, the associated failures have motivated a broader examination of how the different geometries of the VIMs respond to strong beam-induced electromagnetic fields. Circular and elliptical interconnect RF-finger modules were studied using the standard coaxial stretched-wire method. The intrinsic resonances of the modules were identified as a function of the variation of module length and controlled misalignment by means of a new testbench that enables wide geometry variations while keeping the coaxial wire under constant tension.

The measurements reveal clear differences in the resonant spectra of the various designs and show that small geometric deviations can strongly influence mode frequencies and field localisation. Understanding these behaviours is essential, as the High Luminosity upgrade of the LHC (HL-LHC) foreseen to start operation in 2030 will run with even higher bunch intensities, increasing the likelihood that unfavourable resonant conditions could lead to excessive local power deposition. The results contribute to improved assessment and qualification of VIMs for future high-luminosity operation and support the design and development of novel VIMs for next-generation machines.

INTRODUCTION

With the increase in bunch intensity in the Large Hadron Collider (LHC), beam-induced electromagnetic fields in warm vacuum components have become increasingly significant [1]. In particular, VIMs equipped with RF fingers have shown sensitivity to beam-induced heating, and several cases of mechanical degradation and component failure have been reported [2–4]. Of particular concern are fields in regions behind the RF shielding, where unwanted heating has occurred due to field leakage, leading to failures.

VIMs are mechanically flexible structures designed to accommodate installation tolerances, alignment offsets, and thermal expansion. As a result, the modules may operate under varying installation lengths and transverse misalignments [5]. Since electromagnetic resonances are strongly dependent on geometry, such geometric variations may shift resonant frequencies, alter field localisation, and potentially increase local power deposition [1, 2]. Understanding the dependence of resonance behaviour on module geometry is therefore important for assessing operational risks and for the qualification of VIMs.

The electromagnetic behaviour of the modules was investigated experimentally using the coaxial stretched-wire method, a well-established technique for impedance measurements in accelerator components [6, 7]. This study demonstrates its suitability for resonance measurements to identify hidden or unexpected resonances that are computationally intensive to detect, while verifying the functionality of a vacuum component design. A dedicated test bench was developed to maintain constant wire tension while allowing controlled elongation, compression, transverse misalignment, and variation of antenna coupling. This enables systematic and repeatable characterisation of resonances in LHC VIMs without disassembling the measurement setup between configurations.

The approach is demonstrated on an elliptical and a circular interconnect module, for which preliminary results are reported. Resonance behaviour is characterised with respect to module geometry and measurement configuration, including variations in module length, transverse displacement, and antenna coupling, with emphasis on physical interpretation. The impact of degraded electrical shielding is addressed separately to isolate its influence on the measured response.

EXPERIMENTAL SETUP

Measurement Principle

A thin copper wire stretched along the beam axis forms a coaxial transmission line — wire as inner conductor, module body as outer — supporting beam-like electromagnetic excitation, as shown in Fig. 1.

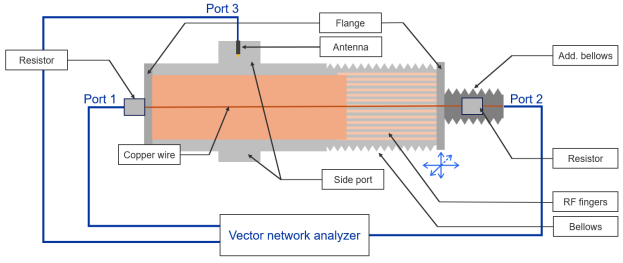

Figure 1: Schematic of the experimental setup. The Blue arrows indicate the adjustable segment.

The stretched wire is connected to a vector network analyzer (VNA) through impedance matching fixtures at both ends of the module. Coupling to the resonances is achieved through the side of the VIM.

* Henrik.ross.gobakken@gmail.com

Test Bench

The incorporation of an additional bellows outside of the interconnecting module was used to enable controlled elongation and compression along the beam axis, transverse misalignment, and reproducible adjustment of the installation length (at the indicated point in Fig. 1). The bellows extends when the module contracts, maintaining a constant overall length and stable tension in the wire. The module is terminated on both sides by flanges with 8 mm apertures for the wire, separating it from the bellows and preserving the electromagnetic boundary conditions.

Comparison measurements performed with and without the additional bellows showed no observable differences in the measured response. This is consistent with its small inner diameter (16 mm), corresponding to a cutoff frequency of 11 GHz, well above the measured frequency range. It therefore does not affect the resonances below the module cutoff (1.4 GHz for the elliptical module, ID 128/53 mm, and 1.6 GHz for the circular ID 110 mm module).

Antenna Configuration

The influence of the antenna configuration on the measured response was investigated using probes with different coupling mechanisms. A straight probe with an insertion length of 5 cm was employed for capacitive coupling, predominantly probing the local electric field. This length provided the most consistent and well-resolved spectral response, and only modes with significant electric field amplitude at the antenna position were observed. Inductive coupling was investigated using a loop probe, which is primarily sensitive to the magnetic field component. The loop opening was oriented both parallel and perpendicular to the module axis to probe different magnetic field components at the measurement location.

By comparing the responses obtained from the straight probe and the loop probe at different positions and orientations, information on the spatial distribution and nature of the resonant modes can be inferred. This approach allows distinguishing between modes with dominant electric or magnetic field components and provides insight into their localisation within the structure.

RESULTS

Baseline Resonance and Displacement Effects

Figure 2 shows the measured frequency spectrum at installation length as well as the normalized beam spectrum for the LHC (filling scheme: 25 ns_2748b_2736_2258_2374_288 bpi_12 inj[1]),generated via BIHC [8], and the effects of controlled elongation and compression. Measurements at LHC installation length for the elliptical configuration show resonance peaks in good agreement with simulations [9, 10]. Several resonance peaks intersect with beam spectral lines. These lines are uniformly spaced across the frequency range, but their amplitudes are higher at low frequencies, leading to stronger beam-driven excitation in this region. Resonances below 1 GHz are therefore of particular concern, as they fall within the region of strongest beam excitation. The cutoff frequency of the structure has been modelled to be approximately 1.4 GHz, indicating that these modes lie well within the region relevant for beam interaction [9].

Systematic shifts in resonant frequencies are observed under controlled geometric deformation: elongation shifts resonances to lower frequencies, while compression shifts them upward. This behaviour follows cavity scaling, where resonant frequencies are inversely proportional to the effective electrical length of the structure, approximated by $f \propto \frac{c}{2L} \cdot n$, with L the characteristic length and n the mode index. This confirms that the observed modes are governed primarily by the global geometry. For the first dominant peak, the frequency shift between the fully compressed and fully elongated configurations is approximately 40 MHz (with variations between modes). This matches the spacing of the beam spectral lines (also 40 MHz), implying that an elongation/compression cycle of approximately 4 cm will inevitably produce overlap with beam spectral peaks.

Transverse misalignment produces only minor frequency shifts and limited amplitude variation. In the low-frequency range (around 1 GHz), the response remains largely unchanged, indicating low sensitivity of these modes to transverse offsets.

Small geometric variations due to installation tolerances or thermal effects can therefore shift resonances into stronger overlap with beam spectral lines, increasing impedance and heating risk.

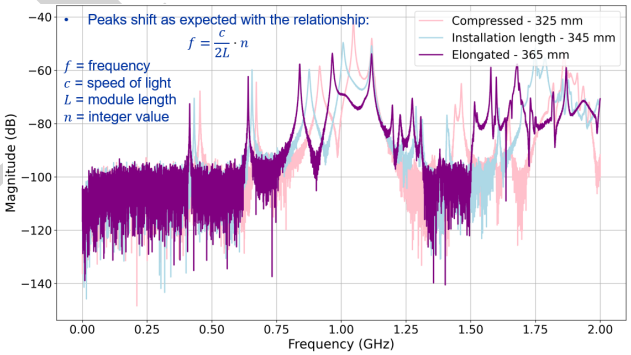

Figure 2: Resonance spectra of the elliptical DN150 module (ID128/53 configuration) measured with a straight 5 cm insertion antenna, including the effects of elongation and compression. The normalized Gaussian beam spectrum for the LHC is shown for comparison.

Field Configuration Testing

To probe the spatial field distributions of the resonant modes, two complementary measurements were performed: rotation of the elliptical module relative to a straight probe antenna, and substitution of the probe with a magnetic loop antenna in two orientations. Figure 3a compares spectra

[1] Fill scheme notation: {bunch spacing}_{bunches per beam}_{IP1/5}_{IP2}_{IP8}_{trainlength}_{injections per beam}.

with the straight probe at the flat side (short-axis) versus the tapered end (long-axis) of the ellipse. In the short-axis configuration, the first resonance near 0.42 GHz is approximately 15 dB stronger, while the second resonance near 0.66 GHz is strongly suppressed. Both observations agree with the simulated electric field distributions (red: maxima, blue: minima; insets adapted from [9]).

Figure 3b shows the same long-axis configuration measured with a loop antenna in parallel and perpendicular orientations. The perpendicular orientation, where the loop normal is aligned longitudinally, yields stronger coupling for both resonances. By Faraday's law, the stronger coupling in the perpendicular orientation indicates that the magnetic flux is predominantly aligned along the module axis, consistent with azimuthally circulating magnetic fields in the dominant modes. The parallel orientation intercepts far less flux, consistent with its weaker response. Due to manufacturing tolerances, the loop is not perfectly parallel or perpendicular, and a more ideal orientation may further suppress the peaks observed in the parallel configuration.

Together, the rotation sensitivity and loop-antenna orientation dependence provide mutually consistent experimental evidence for the simulated field configurations. This demonstrates that further development of this measurement approach could enable systematic experimental mapping of field distributions within the interconnect module, directly supporting identification of RF heating risks.

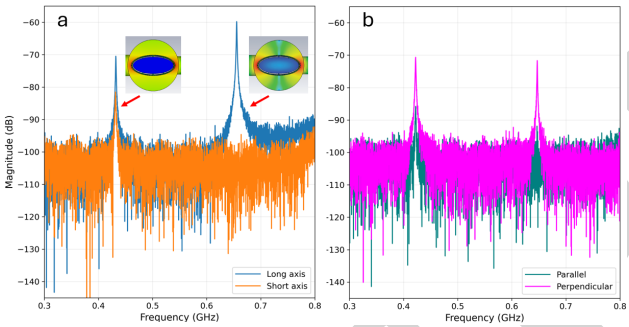

Figure 3: Measured spectra comparing in (a) electric field distribution in two module orientations, with simulated electric field distributions as insets, taken from [9], and in (b) magnetic field via the loop antenna, in long-axis configuration.

Compromised Contact Conditions

To assess the sensitivity of the measurement to contact quality, Kapton foil was inserted between the RF fingers and the transition tube of the circular module to degrade electrical contact, then removed sequentially to restore it without disassembly. Representative spectra are shown in Fig. 4 for four contact conditions: 3/4, 1/2, and 1/4 of the fingers obstructed, and fully restored.

As contact improves, the lowest dominant mode shifts monotonically upward from approximately 0.25 GHz to 0.36 GHz, while higher-frequency modes show a general reduction in amplitude. This suggests that capacitive gaps may modify the effective boundary conditions, shifting resonant frequencies and altering mode amplitudes. Upon full restoration, the two lowest modes merge into a single feature with a more pronounced amplitude reduction than seen between intermediate steps. Poor electrical contact therefore introduces resonances and shifts existing ones toward lower frequencies, where beam spectral power density is higher. The elevated field amplitudes under compromised contact indicate stronger localised field and increased power deposition risk. Good contact suppresses these trapped modes, reducing both amplitude and heating risk.

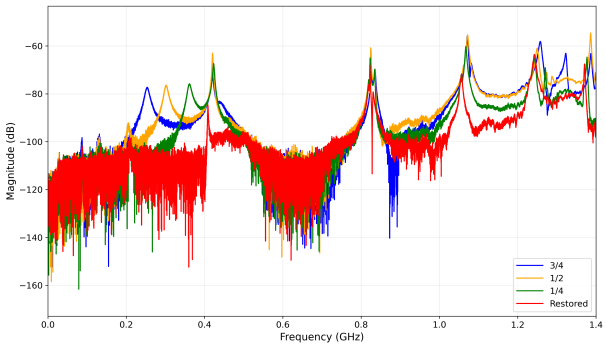

Figure 4: Spectra for four contact conditions: RF fingers with 3/4, 1/2, and 1/4 obstruction, and fully restored contact.

CONCLUSION

The presented measurement setup has proven to be an effective tool for electromagnetic characterisation of VIMs. It enables identification of unexpected resonances that would be difficult to detect through simulation alone, particularly for complex geometries and assembly-dependent effects. Beyond resonance detection, the measurements provide experimental validation that devices behave electromagnetically as assumed during design, construction, and assembly. The sensitivity to mechanical variations further confirms the setup's capability to reveal contact-, alignment-, and deformation-induced electromagnetic effects. An important practical advantage is the rapid testing capability, enabling efficient screening of components prior to installation. As such, the setup represents a valuable diagnostic and verification tool, complementing numerical simulations and reducing the risk of unforeseen impedance, resonance, or heating issues during LHC operation.

REFERENCES

[1] B. Salvant *et al.*, "Beam Induced Heating", in *Proc. 3rd Evian workshop on LHC beam Operation*, Evian les Bains, France, Dec. 2011, pp. 157–163. https://cds.cern.ch/record/1975499

[2] E. Métral *et al.*, "Lessons Learned and Mitigation Measures for the CERN LHC Equipment with RF Fingers", in *Proc. IPAC'13*, Shanghai, China, May 2013, paper TUPWA042, pp. 1802–1804.

[3] O. Kononenko, F. Caspers, A. Grudiev, E. Métral, and B. Salvant, "Impedance Studies for VMTSA Module of LHC

Equipped with RF Fingers", in *Proc. IPAC'13*, Shanghai, China, May 2013, paper TUPWA043, pp. 1805–1807. .

[4] C. Antuono *et al.*, "Impact of high-intensity LHC beam operation on warm vacuum modules", *Phys. Rev. Accel. Beams*, vol. 28, no. 4, p. 041001, Apr. 2025. doi:10.1103/PhysRevAccelBeams.28.041001

[5] R. Veness *et al.*, "Beam Vacuum Interconnects for the LHC Cold Arcs", in *Proc. PAC'99*, New York, NY, USA, Mar. 1999, paper TUA114, pp. 1339–1341.

[6] F. Caspers, "Impedance Determination from Bench Measurements", CERN, Geneva, Switzerland, Rep. CERN-PS-2000-004-RF, Jan. 2000. https://cds.cern.ch/record/437306

[7] V. G. Vaccaro, "Coupling Impedance Measurements: An Improved Wire Method", INFN, Istituto Nazionale di Fisica Nucleare, Rep. INFN/TC-94/023, 1994. https://cds.cern.ch/record/276443

[8] L. Sito, F. Giordano, G. Rumolo, B. Salvant, C. Zannini, and E. de la Fuente, "A Python Package to Compute Beam-Induced Heating in Particle Accelerators and Applications", in *Proc. HB'23*, Geneva, Switzerland, Oct. 2023, pp. 611–614. doi:10.18429/JACoW-HB2023-THBP52

[9] M. Dissanayake, "Impedance Studies on the LHC Interconnect Modules", Master's thesis, CERN, Geneva, Switzerland, Aug. 2024. https://repository.cern/records/n34c4-sgc37

[10] C. Antuono *et al.*, "Beam impedance investigation of the elliptical interconnecting vacuum modules of the LHC and prospect for HL-LHC", in *Proc. IPAC'25*, Taipei, Taiwan, Jun. 2025, pp. 2141–2144. doi:10.18429/JACoW-IPAC2025-WEPM075